JOURNAL OF COMPUTATIONAL PHYSICS 95, 195–211 (1991)

Heat Flow between Species in One-Dimensional Particle Plasma Simulations

WILLIAM S. LAWSON

Courant Institute, New York University, 251 Mercer Street, New York, New York 10012

AND

PERRY C. GRAY

Department of Physics and Astronomy, Dartmouth College, Hanover, New Hampshire 03755

Received August 7, 1989; revised March 19, 1990

The rate of heat flow from one one-dimensional particle species to another is studied using the theory worked out by Eldridge and Feix (*Phys. Fluids* **6**, 398 (1962)). Assuming initial Maxwellian distributions, some approximate formulas are derived which, though still somewhat complex, should be of use to simulators. The results of the theory are tested via simulation using a standard code (A. B. Langdon's ES1 (Langdon and Birdsall, *Plasma Physics via Computer Simulation*, McGraw–Hill, New York, 1985)). The results indicate that heat flow between species is often quite rapid when the real (not necessarily the intended) temperatures are different, and is therefore a serious hazard. Reducing the number of grid cells per Debye length does not seem to reduce the rate of heat flow significantly over the range of grid cell sizes considered. In two and three dimensions the same effect exists, but the magnitude of the effect is not calculated here.

I. INTRODUCTION

Several common practices have arisen in plasma simulation work which rely on varying the charge ratios between particles (of the same or differing species) in an unphysical way. One such practice is to model a minority species by subdividing it into a large number of particles, i.e., replace a small number of particles by a large number of particles each of which have the same charge-to-mass ratio, but a fraction of the charge and mass of the particle one actually wants to simulate [1, 2]. Another practice is to vary the weights of particles in time [3]. Most of these practices have been adopted in order to reduce noice, but they raise the concern that heat flow between species can interfere with the correct results of the simulation.

It is easy to see the origin of this concern. The true thermodynamic temperature

0021-9991/91 $3.00

of any distribution is $T = mv_t^2$. If the particles of a distribution are subdivided without altering their thermal velocities (which are usually chosen to reflect some desired resonant interaction), then the temperature of the subdivided species falls, and heat will flow from the other species (assuming they are intended to be at the same temperature). Researchers often overlook this fact because they are thinking in terms of Vlasov theory, in which temperature plays no role. Another source of confusion is the common idea that each simulation particle is meant to represent many real particles. A direct corollary of this idea would seem to be the principle that it should not matter how many real particles a given simulation particle is supposed to represent, but the above argument shows that thermodynamic arguments invalidate this simple picture of simulation.

While the existence of this heat-flow effect is indisputable, it may not be of concern if the rate of heat flow is small enough. This heat flow rate is of central importance and has not been previously investigated in depth.

Using the remarkable work of Eldridge and Feix [4], we will derive an expression for this heat flow rate, interpret the terms physically, derive some approximate formulas, and finally test the theory with simulations. The theory and its interpretations appear in Section II, Section III contains the simulation results, and Section IV discusses the consequences of this effect for plasma simulation.

II. Theory

The relevant work of Eldridge and Feix is contained in the appendix to Ref. [4]. Since this reference is readily available, it would serve no purpose to repeat their derivation here, but several comments on it are essential, first, because we have chosen slightly different notation that better illuminates the results in the present context and, second, because of some points and minor oversights.

The first point is merely awkward. Eldridge and Feix introduced *arbitrary* reference values for charge (denoted as σ) and number density (denoted as n_0). These led to a non-standard definition of the plasma frequency $\omega_{p\alpha}$, and the introduction of a normalized charge $z_\alpha = \sigma_\alpha/\sigma$. (It may have been these complications which led to the accidental omission of factors of z_α^2 in the definitions of F and f, and in their Eq. (28), which is their final result.) In our work, the standard definition of plasma frequency is used, and no arbitrary normalization factors are introduced.

The other point is clarified in the text of their article, but not in the appendix. The final result of Eldridge and Feix contains a function denoted as an arc tangent of a ratio of two functions while what was intended was something slightly different. The strictly correct expression is an *argument* function of the two functions. The arc tangent function ranges from $-\pi/2$ to $\pi/2$, but the argument function ranges from $-\pi$ to π, and this is essential.

The final result of Eldridge and Feix, when put in standard notation, is

$$\frac{\partial f_\alpha}{\partial t}=\frac{1}{2\pi}\frac{\omega_{p\alpha}^2}{n_\alpha}\frac{\partial}{\partial v}\left\{\left[f_\alpha-\frac{1}{m_\alpha}\frac{\partial f_\alpha/\partial v}{\partial f/\partial v}F\right](-\arg(\psi,\pi\,\partial f/\partial v))\right\}, \tag{1}$$

where f_α is the distribution function for species α normalized such that its integral is one,

$$f=\sum_\alpha \omega_{p\alpha}^2 f_\alpha \tag{2}$$

$$F=\sum_\alpha m_\alpha \omega_{p\alpha}^2 f_\alpha \tag{3}$$

and

$$\psi(v_1)=\mathrm{PV}\int_{-\infty}^{\infty}\frac{\partial f(v_2)/\partial v_2}{v_1-v_2}\,dv_2. \tag{4}$$

This formula assumes more physical meaning if it is realized (as was pointed out by Langdon and Birdsall [5]) that

$$-\arg(\psi,\pi\,\partial f/\partial v)=\arg(\chi(k,kv)),$$

where the arg function is now to be interpreted as the phase angle in the complex plane, and χ is the dielectric susceptibility. Because of the form of χ, this expression is independent of k. The only factor influencing f at a given velocity that depends on the values of f at any other velocities is the arg function. One can interpret this as particles interacting only with particles at or near the same velocity, but interacting through the electric field as modified by the entire plasma.

Dawson showed heuristically that the time scale for velocity drag and diffusion should be of order N_D/ω_p, where N_D is the number of particles per Debye length [6]. This scaling can be deduced directly from Eq. (1), but Eq. (1) does not provide any simple answer for the constant of proportionality.

One exact prediction of Eq. (1) is that a single species plasma does not evolve at all, regardless of its distribution. In fact, Dawson showed that a single species relaxes to a Maxwellian on a time scale proportional to N_D^2/ω_p [7]. In general, evolution on a time scale of N_D/ω_p is to be expected, but when two or more species are involved, there are several space and time scales available, so that it is necessary to do some more estimation to find a useful scale rule.

It is possible to generalize the single-species result to the following statement: *if $f_\alpha f_\beta=0$ for all $\alpha\neq\beta$ (i.e., the distribution functions do not overlap), then the distribution functions do not evolve to first order in N_D*. A more general constraint is pointed out by Birdsall and Langdon:

$$\frac{\partial}{\partial t}\sum_\alpha n_\alpha m_\alpha f_\alpha=0. \tag{5}$$

This is a powerful constraint, but not immediately useful except in the special cases noted above.

One important contribution toward understanding heat flow effects was made by Okuda and Birdsall [8], who evaluated the drag diffusion coefficients for one-, two-, and three-dimensional plasmas of particles of non-zero extent. This is equivalent to the evaluation of Eq. (1) in the special case of isothermal Maxwellian distributions, but with the important addition of non-zero size particles. Their results, to which we will return in the simulation section, showed a reduction in heat flow when particle sizes were on the order of a Debye length. We will limit ourselves to the case of point particles, but investigate heat flow between differing distributions and test the results by simulation.

Equation (1) is somewhat intimidating, but choosing Maxwellian distributions for each species as a special case simplifies it immensely. Driftless Maxwellians are not the only case of interest, but they are the most common, and it will be seen that they introduce enough complexity already as to make it impossible to give a *simple* rule of thumb. To simplify the algebra, let $k_{D\alpha} = \omega_{p\alpha}/v_{t\alpha}$ be the inverse of the Debye length for species α, then the first term in brackets in Eq. (1) becomes

$$\left[f_\alpha - \frac{\partial f_\alpha/\partial v}{m_\alpha\, \partial f/\partial v} F\right] = \frac{f_\alpha}{T_\alpha}\left[T_\alpha - \frac{\sum_\beta T_\beta k_{D\beta}^2 f_\beta}{\sum_\beta k_{D\beta}^2 f_\beta}\right]$$
$$= \frac{f_\alpha}{T_\alpha} \sum_\beta (T_\alpha - T_\beta) \frac{k_{D\beta}^2 f_\beta}{\sum_\gamma k_{D\gamma}^2 f_\gamma}, \tag{6}$$

where $T_\alpha = m_\alpha v_{t\alpha}^2$ is the true (as opposed to intended) temperature of species α. Furthermore, substituting the usual expression for the susceptibility of a plasma in terms of the standard plasma dispersion fucntion Z [9] shows that for Maxwellian distributions,

$$-\arg(\psi, \partial f/\partial v) = \arg\left(-\sum_\alpha k_{D\alpha}^2 Z'\left(\frac{v}{\sqrt{2}\, v_{t\alpha}}\right)\right), \tag{7}$$

where the argument function is understood to be the angle in the complex plane and prime denotes derivative with respect to the argument of the Z function.

Finally, since the instantaneous heat flow should suffice for an estimate, take the second moment of (1), i.e., multiply by $n_\alpha m_\alpha v^2/2$ and integrate (integrating once by parts). This yields

$$\left.\frac{d\mathscr{E}_\alpha}{dt}\right|_{t=0} = \frac{1}{2\pi}\sum_\beta (T_\beta - T_\alpha) \int_{-\infty}^{\infty} v \left[\frac{k_{D\alpha}^2 f_\alpha \cdot k_{D\beta}^2 f_\beta}{\sum_\gamma k_{D\gamma}^2 f_\gamma}\right]$$
$$\times \arg\left(-\sum_\gamma k_{D\gamma}^2 Z'\left(\frac{v}{\sqrt{2}\, v_{t\gamma}}\right)\right) dv. \tag{8}$$

The symmetry of this formula is evident, and it is also now possible to make an important observation regarding the term in brackets: it is always less than the minimum of $k^2_{D\alpha}f_\alpha$ and $k^2_{D\beta}f_\beta$. This upper bound will be useful in formulating approximations. The obvious physical interpretation of this term is that the particles of a given species at a given energy will receive energy (or lose it) in proportion to their numbers and charge strength (and weighted by the arg function).

The general shape of the argument function is not obvious, but can be seen by plotting the real and imaginary parts of the Z' function (see Fig. 1). Figure 2 shows the argument function for a two-species plasma for $v_{t1} = v_{t2}$ and for $v_{t1} = 10v_{t2}$. As can be seen, there is some fine structure when the thermal velocities are different which cannot be ignored.

Equation (8) can be written in the form

$$n_\alpha \left.\frac{dT_\alpha}{dt}\right|_{t=0} = \sum_\beta (T_\beta - T_\alpha) C_{\alpha\beta}, \tag{9}$$

where

$$C_{\alpha\beta} = \frac{1}{\pi}\int_{-\infty}^{\infty} v \left[\frac{k^2_{D\alpha}f_\alpha \cdot k^2_{D\beta}f_\beta}{\sum_\gamma k^2_{D\gamma}f_\gamma}\right] \arg\left[-\sum_\gamma k^2_{D\gamma} Z'\left(\frac{v}{\sqrt{2}\,v_{t\gamma}}\right)\right] dv \tag{9}$$

and clearly

$$C_{\alpha\beta} = C_{\beta\alpha}.$$

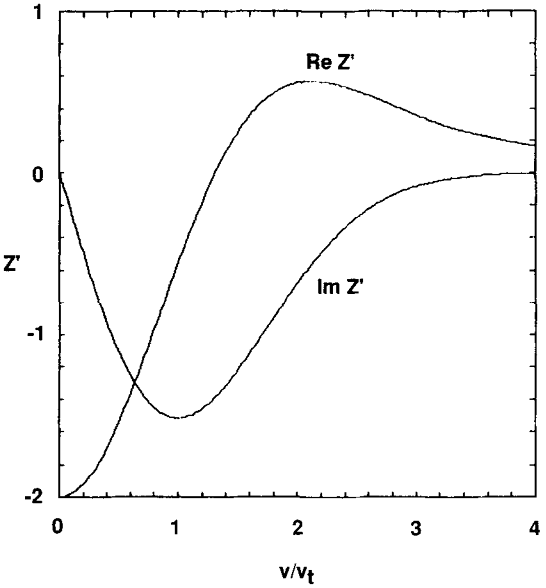

FIG. 1. Real and imaginary parts of Z' function for real argument.

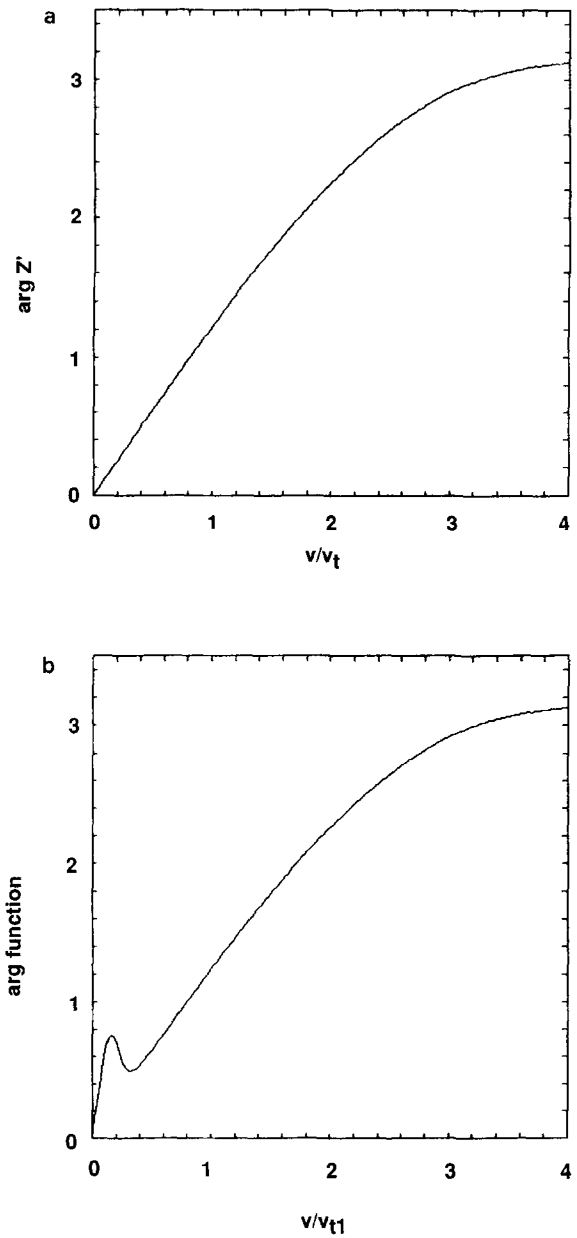

FIG. 2. (a) Argument function of $-Z'$. (b) Argument function of $-Z'(v/\sqrt{2}) - Z'(10v/\sqrt{2})$.

Since the heat flow is evidently between pairs of species (though mediated by the dielectric of the entire plasma), it should be most illuminating to consider just two species. The time we would like to estimate is the time in which one of the distributions changes temperature significantly. A reasonable formal definition of this time of interest (call it τ) is the minimum over species of

$$\tau_\alpha = \left| \frac{1}{T_\alpha} \frac{dT_\alpha}{dt} \right|^{-1}. \tag{11}$$

Since the energy flow rates are the same between two species, comparison with Eq. (9) shows that the species with the minimum energy, or nT will have the minimum τ. Unfortunately, examination of the relations between n, T, k_D, and v_t show that all four can be chosen independently, so any approximation will have at least these four parameters in it.

Let us now specialize to the case of only two species which we will label species a and species b. Since the formula for $C_{\alpha\beta}$ has only two parameters per species and has the most complex form, it is the natural starting point for simplification. We shall divide the evaluation of C_{ab} into four regimes: (I), $v_{ta} = v_{tb}$; (II), $v_{ta} \ll v_{tb}$ and $k_{Da} \gg k_{Db}$; (III), $v_{ta} \ll v_{tb}$ and $k_{Da} \sim k_{Db}$; and (IV), $v_{ta} \ll v_{tb}$ and $k_{Da}^2/v_{ta} < k_{Db}^2/v_{tb}$. This division is motivated by the approximation to be used for case II. The gaps between these regimes are of interest, but have a behavior intermediate between those given, so application of the complete Eq. (8) is necessary if a better estimate is desired than the worst of the closest cases given.

Case I allows the simplification

$$\begin{aligned} C_{ab} &= \frac{1}{\pi} \frac{k_{Da}^2 k_{Db}^2}{k_{Da}^2 + k_{Db}^2} \int_{-\infty}^{\infty} v f(v) \arg\left[-Z'\left(\frac{v}{\sqrt{2}\, v_t}\right)\right] dv \\ &= 0.36582 \times \frac{k_{Da}^2 k_{Db}^2}{k_{Da}^2 + k_{Db}^2} v_t \\ &= 0.36582 \times \frac{\omega_{pa}^2 \omega_{pb}^2}{\omega_{pa}^2 + \omega_{pb}^2} \frac{1}{v_t}. \end{aligned} \tag{12}$$

As a gross estimate of how important this should be in a real simulation, let us take $\omega_{pa} = \omega_{pb}$; then using our definition of τ,

$$\tau \approx 5 \frac{n\lambda_D}{\omega_p} \left| 1 - \frac{T_b}{T_a} \right|^{-1}. \tag{13}$$

This is an alarmingly short time in the context of most simulations if the temperature ratio deviates much from unity. This is also what one would expect from purely dimensional arguments, so the other cases can be expected to scale similarly, though perhaps with different species dominating the time and space scales.

Case II is the most complex one, and the most likely. The strategy of the approximation can be understood from Fig. 3. Since the term in brackets in Eq. (8) is always less than the minimum, it can be seen that a good approximation, when the thermal velocities are highly disparate, is that this term can be replaced by $f_b(0)$ for $v < v_c$, and by zero for $v > v_c$, where v_c is roughly the point at which the two distribution functions, multiplied by their respective k_D's, cross. Some simple algebra shows that

$$v_c \approx v_a \sqrt{2 \ln \frac{k_{Da}^2 v_{tb}}{k_{Db}^2 v_{ta}}}. \tag{14}$$

A further approximation is to approximate the arg function by a straight line with the same slope at the origin. For $k_{Db} \ll k_{Da}$, the second Z' term can be ignored completely, leaving the curve of Fig. 2a, which is not far from a straight line in most of the region of interest, but the approximation can be expected to be a bit high. The imaginary part of the $Z'(\xi)$ function divided by its real part is $\sqrt{\pi}\,\xi$ for small ξ, so

$$C_{ab} \approx \frac{1}{\pi} \int_{v_c}^{v_c} v k_{Db}^2 f_b(0) \sqrt{\frac{\pi}{2}} \left[\frac{kDa^2/v_{ta}}{k_{Da}^2 + k_{Db}^2} \right] v\, dv$$
$$= \frac{1}{3\pi} \frac{k_{Da}^2 k_{Db}^2}{k_{Da}^2 + k_{Db}^2} \frac{v_{ta}^2}{v_{tb}} \left[2 \ln \frac{k_{Da}^2 v_{tb}}{k_{Db}^2 v_{ta}} \right]^{3/2}. \tag{15}$$

This is disappontingly complex for a rule of thumb, but, as will be shown, the functional dependence is borne out by numerical integration of Eq. (8). The estimate is roughly a factor of 1.5 too high, though. Fortunately, the logarithm can be estimated with relative case, and exact evaluation is not the goal.

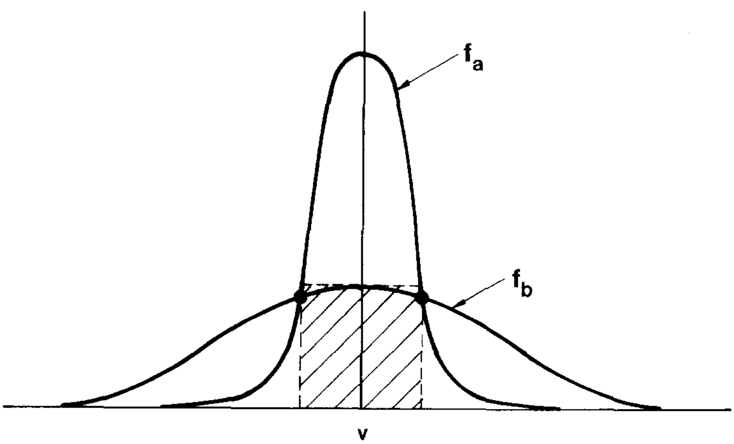

FIG. 3. Since $f_a f_b/(f_a + f_b) \leqslant \min(f_a, f_b)$, shaded area can be used as an approximation when thermal velocities are very different.

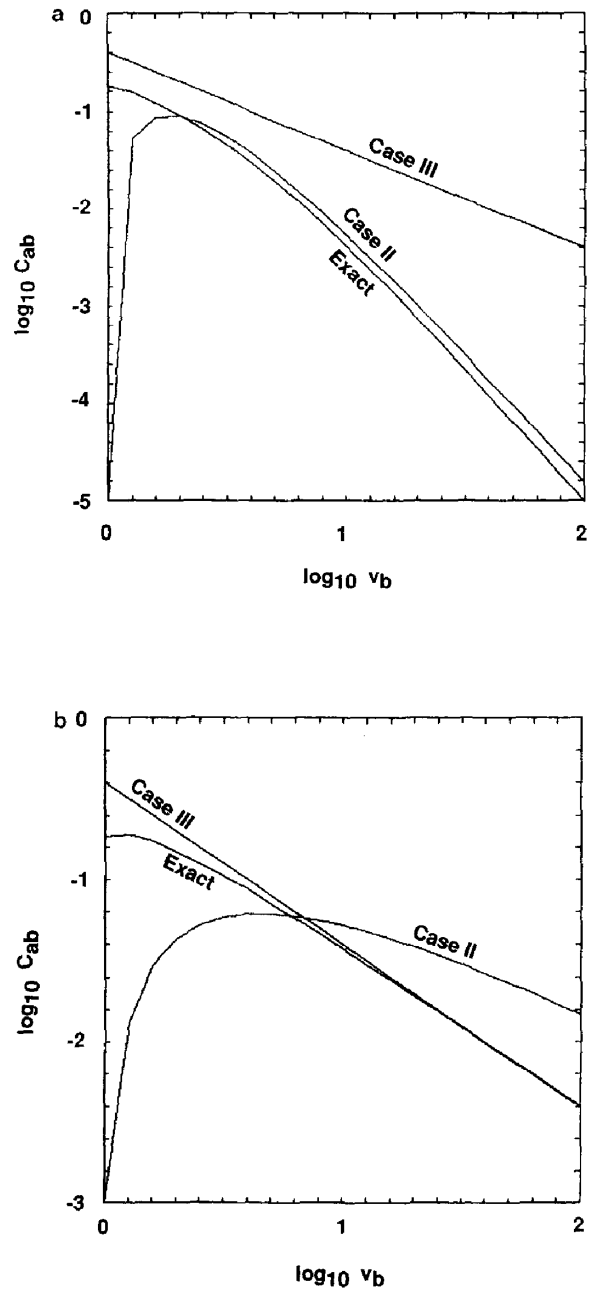

FIG. 4. Exact curve for case II versus approximations for cases II and III. (b) Exact curve for case III versus approximations for cases II and III.

In case III, as in case II, the arg function must be approximated, but now both Z' terms must be taken into account. The real part of $Z'(\xi)$ dies away roughly as $\exp(-\xi^2)$, so the real part of $k_{Da}^2 Z'(v/\sqrt{2}\, v_{ta})$ can be neglected. This is not very good for small v, but the factor of v in the integrand reduces the importance of small v. The imaginary part of the Z' term for species b can also be neglected, since it is inversely proportional to v_{tb}, so

$$C_{ab} \approx \frac{1}{\pi} \int_{-\infty}^{\infty} v \frac{1}{\sqrt{2\pi}\, v_{tb}} k_{Db}^2 \cdot \sqrt{\frac{\pi}{2}} \frac{k_{Da}^2}{k_{Db}^2} \frac{v}{v_{ta}} \exp\left(-\frac{v^2}{2v_{ta}}\right) dv$$
$$= \frac{1}{\sqrt{2\pi}} k_{Da}^2 \frac{v_{ta}^2}{v_{tb}}. \tag{16}$$

Figure 4 shows calculations of two cases with the exact integral and the approximations for both case II and case III. It can be seen that both approximations have their regions of validity, and both are necessary.

In case IV, $k_{Da}^2 f_a < k_{Db}^2 f_b$ for all v, so it can replace the term in brackets in Eq. (8). Making the same approximation for the arg funtion as in case II,

$$C_{ab} \approx \frac{1}{\pi} \int_{-\infty}^{\infty} v k_{Da}^2 f_a(v) \sqrt{\frac{\pi}{2}} \left(\frac{k_{Da}^2/v_{ta} + k_{Db}^2/v_{tb}}{k_{Db}^2} \right) v\, dv$$
$$= \frac{1}{\sqrt{2\pi}} k_{Da}^2 v_{ta}^2 \left(\frac{1}{v_{tb}} + \frac{k_{Da}^2}{k_{Db}^2 v_{ta}} \right)$$
$$\leqslant \sqrt{\frac{2}{\pi}} k_{Da}^2 \frac{v_{ta}^2}{v_{tb}}$$
$$= \sqrt{\frac{2}{\pi}} \frac{\omega_{pa}^2}{v_{tb}}. \tag{17}$$

Each of these four cases scales as some dimensionless number times some frequency like a plasma frequency divided by some length like a Debye length, and so the heating time will scale like

$$\tau_a = \left| \frac{T_b}{T_a} - 1 \right|^{-1} \frac{n_a}{C_{ab}} \sim \left| \frac{T_b}{T_a} - 1 \right|^{-1} \cdot \frac{\langle N_{Da} \rangle}{\langle \omega_p \rangle}. \tag{18}$$

The individual cases must be consulted to determine which Debye length and plasma frequency (perhaps with a ratio of thermal speeds multiplied in) should be used.

III. Simulation Results

Since the different mathematical regimes necessary for construction of useful approximations ought to have some physical significance as well, they are logical

TABLE I

Run Parameters

Set	1	2	3	4	5
Case	I	I	II	III	I
Length	25	25	25	25	25
Time steps	4000	1000	4000	4000	4000
Grid cells	128	128	128	128	32–256
N_{pa}	1280–10,240	5120	5120	5120	5120
N_{pb}	12,800	5120	5120	5120	12,800
v_{ta}	1	1	0.125–0.75	0.1–0.5	1
ω_{pa}	1	0.1–0.5	1	0.1–0.5	1
q_a/m_a	1	0.01–0.25	1	1	1
Figure	5	7	8	9	10

Note. Simulation parameters; in addition, $\varepsilon_0 = 1$, $\Delta t = 0.05$, $v_{tb} = 1$, $\omega_{pb} = 1$, and $q_b/m_b = -1$ for all runs.

choices for simulation tests. Therefore, test simulations were run in three of the four regimes (case IV) being omitted, as it seems to be a less sensitive case). Additional runs were performed in order to test the effect of grid spacing. For consistency with the previous section, the second species (to be referred to as species b) was given unit thermal velocity and plasma frequency, while species a was given *smaller* thermal velocity or plasma frequency. Both species were assumed to have the same

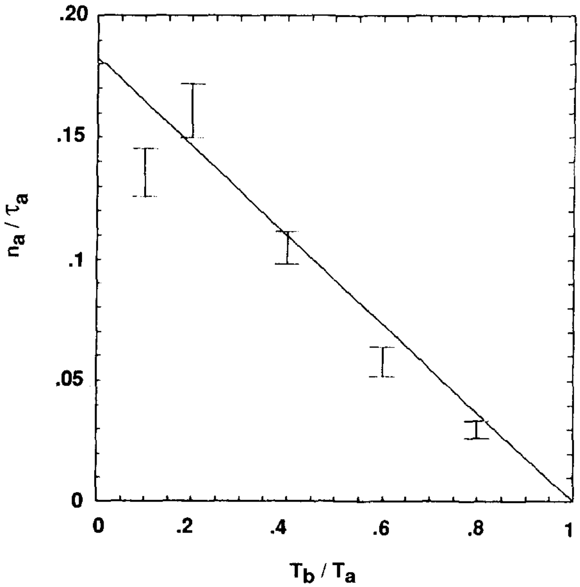

FIG. 5. Simulation results for equal thermal velocities and plasma frequencies (also equal charge-to-mass ratios).

charge-to-mass ratio (except in the simulations of case II—in order to create a temperature difference with equal numbers of particles). The complete simulation parameters are shown in Table I. The particles were loaded uniformly in position and randomly in velocity; experience has shown that this arrangement leads most quickly to the natural level of fluctuations. In all cases, the simulation results are compared with the exact Eq. (1) evaluated numerically.

In the first set of runs (a special case of case I in the previous section), the two species are taken to have identical plasma parameters, except for the sign of their charge density, and the number of particles (i.e., only the temperatures differ). Therefore, the theoretical relaxation rate is a straight line when plotted against the temperature ratio. In these runs, the number of particles per Debye length of the first species is a constant 512, while the number of particles per Debye length of the second species is varied from 512 down to 51.2. The simulation results are shown in Fig. 5, and agree reasonably well with the numerically determined values. The error bars are eyeball estimates taken from the graphs. Temperature ratios near unity are avoided because of severe noise problems. A typical graph is shown in Fig. 6. The noise level in this graph is about average, so that for the noisier runs it is possible that the error is actually somewhat larger than that plotted. The disparity between the points at $T_a/T_b = 0.1$ and 0.2 (barring the possibility that the predictions of the theory are incorrect) is the clearest example of this (these were the two noisiest runs). The disparity itself is likely to be a better indication of the overall accuracy of the data points than the plotted error bars. In general, the errors in C_{ab} are greatest when the number of particles is smallest and when the heat flow is smallest (i.e., when the two distributions are closest to equilibrium).

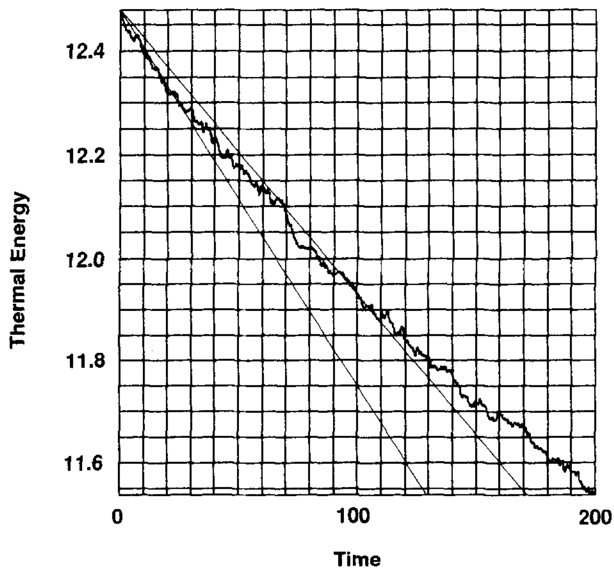

FIG. 6. Representative energy history with bounding slopes. In this case, $v_a = 0.5v_b$ and $\omega_{pa} = \omega_{pb}$.

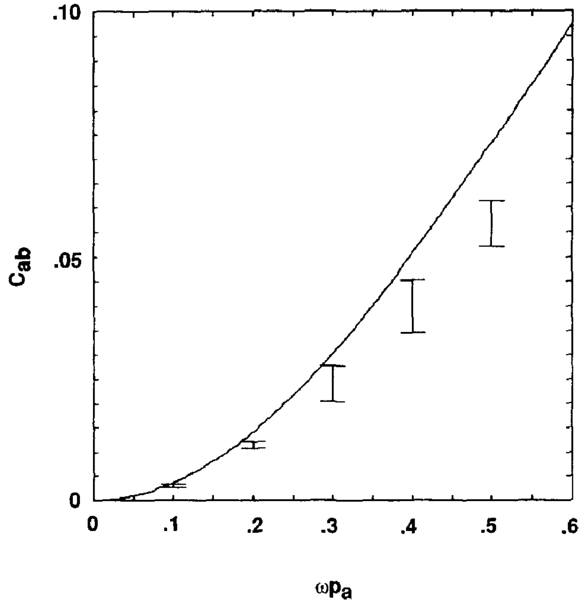

FIG. 7. Simulation results for $v_a = v_b$, $N_a = N_b$, and $q_a = q_b$ (unequal charge-to-mass ratios).

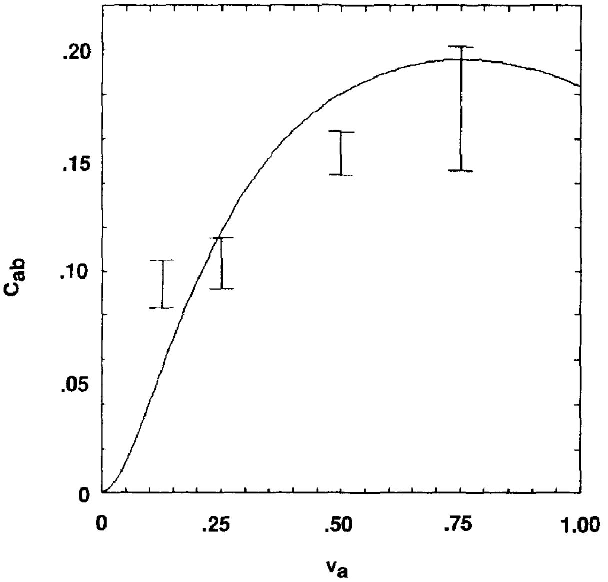

FIG. 8. Simulation results for $\omega_{pa} = \omega_{pb}$, $N_a = N_b$, and $q_a = q_b$.

A more thorough test of case I is the second set of simulations (see Fig. 7). In these simulations the thermal velocities are held equal, and the charge per particle is the same for both species, but now the plasma frequencies are varied (again with 204.8 per Debye length for species one). Again, temperature ratios near unity have not been plotted.

The third set of runs corresponds to case II (see Fig. 8). In this case, the plasma frequencies of the two species are equal, and the thermal velocities are varied for equal numbers of particles. Again species one has 204.8 particles per Debye length, but since the Debye length for species two is decreasing, the grid spacing must be decreased for each run in order to maintain $\Delta x/\lambda_D < 0.2$ for both species. As before, the agreement is reasonably good, except for the smallest ratio of thermal speeds. Inspection of the distribution functions at the end of the runs shows that they are quite different from Maxwellians. If the heating time for the cold species is computed for a ratio of thermal velocities of ten, it is found to be roughly $70/\omega_p$, which is less than the time necessary to measure a reliable slope. Thus it seems that the heating rate is higher because the assumption of Maxwellian distributions broke down before the initial rate of heat flow could be measured.

The fourth set of runs corresponds to case III. This time the Debye lengths are held equal, and the number of particles is held equal at 204.8, meaning that the charge density of species two (and the charge per particle) will be less than that for species one. It is impossible to make the charge densities of the two species equal and opposite in this case without changing the charge-to-mass ratio, but there is no need for the species to have equal and opposite charges. A uniform neutralizing

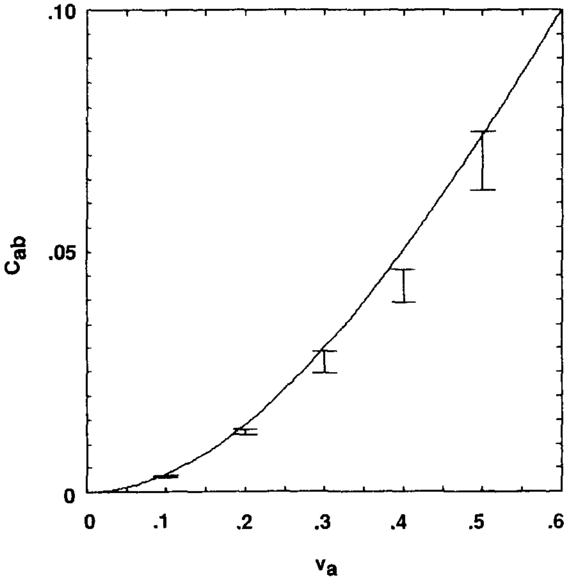

FIG. 9. Simulation results for $\lambda_{Da} = \lambda_{Db}$, $N_a = N_b$, and $q_a = q_b$ (unequal charge densities).

background charge has no effect on the heat flow. The results are shown in Fig. 9, and again they seem to agree with theory.

The fifth and final set of runs duplicate one of the runs from the first set, but at varying values of $\Delta x/\lambda_D$. For convenience, the system length was chosen to be 32 rather than 25, and the number of grid cells per Debye length was chosen successively to be 8, 4, 2, and 1. All the rates seem to be slightly below the prediction (see Fig. 10), but there is a marked decrease in the heat flow rate only for $\lambda_D = \Delta x$, and this is by less than a factor of two. Choosing $\Delta x/\lambda_D > 1$ becomes risky due to increasing self-heating and alteration to the dispersion relation which can even produce instability. There is nothing definitive about this limit, but to exceed it one must be very aware of the many things that can go wrong, so we will not exceed it here. The simulations agree quite well with the one-dimensional result of Okuda and Birdsall [8]. It is worth noting that in two and three dimensions a $\Delta x/\lambda_D$ of unity should give much larger reductions in the heat flow rate (between one and two orders of magnitude).

One statistical feature of the results requires some comment. On the whole, the results tend to be less than the predictions. Several reasons may exist for this. First, the graphical method for determining the error bars favors low estimates if the slope is a decreasing function of time, which was indeed the case in most of the runs. Second, the time step and finitesimal particle size may have a small systematic effect. Two other obvious possibilities are simple coincidence and an incorrect theory. Despite the statistical errors, it is clear that the results are off by a few percent and not orders of magnitude, and this is the important feature in practical terms.

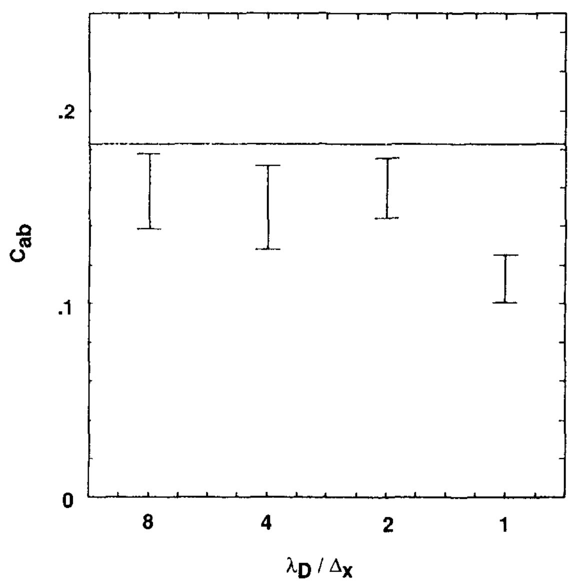

FIG. 10. Results for varying values of $\lambda_D/\Delta x$.

IV. Consequences for Simulation

The theory of Eldridge and Feix, along with the work in Section II of this paper, is nice to have, but it is unlikely that any simulator would want to resort to such a detailed calculation in order to bolster his simulation results. Therefore, aside from the rules of thumb so far derived, the theory is mostly useful in the *character* of its results.

There is one aspect in particular of the results which has great significance for practical tests of simulation accuracy. Consider the practice of representing a minority species by a large number of particles, each of which is much less massive than a particle of the majority species (we will call this practice *particle chopping*, but it is sometimes referred to as the use of superparticles). If the result of a simulation run is that the minority species heats, it is of interest to know whether that heating is physical or numerical. The particular problem may not involve Maxwellians, and the Eq. (1) may not be easy to evaluate for the actual distributions. A numerical test would be desirable.

The time-tested method of determining the effects of non-physical processes in a simulation plasma is to alter the simulation parameters, observing whether different results are thus obtained. In the case of particle chopping, the obvious way of testing the effects of the chopping would be to vary the degree of chopping. Our work, however, shows that this is *not* a good test, since the limit approached is that of zero temperature for the chopped species, while the unchopped species determines the rate of heat flow. The proper way to test for heat flow effects is to chop the *unchopped* (majority) species.

In simulations in which particle chopping does not occur, the heat flow is less likely to be a problem unless the temperature difference between the species is significant. The worst case is, of course, when the temperature difference is such as to bring the thermal velocities closer.

This context of simulation raises an interesting possibility. The judicious use of particle chopping could be used to reduce or remove a temperature difference in a simulation in which one would otherwise exist. Instabilities on a macroscopic scale would still be present (temperature does not enter into the Vlasov theory), but much longer runs would be possible, since the artificially high heat flow has been reduced or eliminated. One such scenario would be that of a high-temperature minority.

V. Summary

The heat flow rate between species of one-dimensional point particles (the sheet model) having Maxwellian distributions has been cast in the form

$$\left.\frac{d\mathscr{E}_\alpha}{dt}\right|_{t=0} = \frac{1}{2}\sum_\beta (T_\beta - T_\alpha)\cdot C_{\alpha\beta}(\omega_{p1}, v_{t1}, \omega_{p2}, v_{t2}, \ldots), \tag{19}$$

where $C_{\alpha\beta} = C_{\beta\alpha}$ are known but rather complex functions of the plasma frequencies and thermal velocities of all the species, using the theory of Eldridge and Feix. From this result approximations for four regimes were derived for the special case of two species. These approximations were tested against the exact expression.

The theory was tested in detail against simulation results with reasonable agreement. It was found that choosing the number of grid cells per Debye length to be small did not reduce the rate of heat flow enough to be of use.

Finally, the practical importance of this work to simulation was assessed, particularly regarding the practice of replacing a few particles of a given species with a large number of smaller particles with the same charge-to-mass ratio (chopped particles). It was concluded that under many circumstances the heat flow between species could be a strong effect and that some care is necessary in making test runs to assess its magnitude.

Acknowledgments

We gratefully acknowledge helpful discussions with professors C. K. Birdsall, M. K. Hudson, and N. F. Otani. This work was supported by U.S. Department of Energy Grant DE-FG02-86ER53223 and NASA Grant NAGW-1652.

References

1. Y. Omura, M. Ashour-Abdalla, R. Gendrin, and K. Quest, *J. Geophys. Res.* **90**, 8281 (1985).
2. D. Winske and M. M. Leroy, *J. Geophys. Res.* **89**, 2673 (1984).
3. M. Kotschenreuther, personal communication.
4. O. C. Eldridge and M. Feix, *Phys. Fluids* **6**, 398 (1963).
5. C. K. Birdsall and A. B. Langdon, *Plasma Physics via Computer Simulation* (McGraw–Hill, New York, 1985), p. 287.
6. J. M. Dawson, *Phys. Fluids* **5**, 445 (1962).
7. J. M. Dawson, *Phys. Fluids* **7**, 419 (1964).
8. H. Okuda and C. K. Birdsall, *Phys. Fluids* **13**, 2123 (1970).
9. B. D. Fried and S. D. Conte, *The Plasma Dispersion Function* (Academic Press, New York, 1961).